

Differentiated Parkinson patient-derived induced pluripotent stem cells grow in the adult rodent brain and reduce motor asymmetry in Parkinsonian rats

Gunnar Hargus^a, Oliver Cooper^a, Michela Deleidi^a, Adam Levy^a, Kristen Lee^a, Elizabeth Marlow^a, Alyssa Yow^a, Frank Soldner^b, Dirk Hockemeyer^b, Penelope J. Hallett^a, Teresia Osborn^a, Rudolf Jaenisch^{b,1}, and Ole Isacson^{a,1}

^aUdall Parkinson's Disease Research Center of Excellence and Center for Neuroregeneration Research, McLean Hospital/Harvard Medical School, Belmont, MA 02478; and ^bWhitehead Institute for Biomedical Research, Massachusetts Institute of Technology, Cambridge, MA 02142

Contributed by Rudolf Jaenisch, July 14, 2010 (sent for review April 15, 2010)

Recent advances in deriving induced pluripotent stem (iPS) cells from patients offer new possibilities for biomedical research and clinical applications, as these cells could be used for autologous transplantation. We differentiated iPS cells from patients with Parkinson's disease (PD) into dopaminergic (DA) neurons and show that these DA neurons can be transplanted without signs of neurodegeneration into the adult rodent striatum. The PD patient iPS (PDiPS) cell-derived DA neurons survived at high numbers, showed arborization, and mediated functional effects in an animal model of PD as determined by reduction of amphetamine- and apomorphine-induced rotational asymmetry, but only a few DA neurons projected into the host striatum at 16 wk after transplantation. We next applied FACS for the neural cell adhesion molecule NCAM on differentiated PDiPS cells before transplantation, which resulted in surviving DA neurons with functional effects on amphetamine-induced rotational asymmetry in a 6-OHDA animal model of PD. Morphologically, we found that PDiPS cell-derived non-DA neurons send axons along white matter tracts into specific close and remote gray matter target areas in the adult brain. Such findings establish the transplantation of human PDiPS cell-derived neurons as a long-term in vivo method to analyze potential disease-related changes in a physiological context. Our data also demonstrate proof of principle of survival and functional effects of PDiPS cell-derived DA neurons in an animal model of PD and encourage further development of differentiation protocols to enhance growth and function of implanted PDiPS cell-derived DA neurons in regard to potential therapeutic applications.

cell replacement therapy | dopaminergic neurons | Parkinson's disease | reprogramming | transplantation

The induced pluripotent stem (iPS) cell technology provides an opportunity to generate cells with characteristics of embryonic stem (ES) cells, including pluripotency and potentially unlimited self-renewal (1). During the past few years, several studies have reported a directed differentiation of iPS cells into a variety of functional cell types in vitro, and cell therapy effects of implanted iPS cells have been demonstrated in several animal models of disease (2, 3).

Reprogramming technology has been applied to derive patient-specific iPS cell lines, which carry the identical genetic information as their patient donor cells. This is particularly interesting for regenerative cell therapy approaches, as differentiated patient-specific iPS cells might be used for autologous transplantation. Patient-specific iPS cell lines have been generated for several diseases, including hematologic (4), metabolic (5, 6), and neurologic disorders (5, 7–9). To model disease in vitro, changes have been obtained in patient-derived iPS cells, which could be modified through the application of chemical compounds during iPS cell differentiation (8, 9) or prevented by gene targeting before iPS cell derivation (4). Furthermore, functional phenotypes such as insulin-producing cells from diabetic patients have been generated from iPS cells in vitro (6), demonstrating that patient-derived iPS cells can constitute a potential source for future clinical applications.

Cell replacement therapy is promising in diseases with a relatively selective cell loss, such as Parkinson's disease (PD), in which dopaminergic (DA) neuron degeneration is responsible for motor symptoms in patients. Several studies have shown that some patients with PD benefit from the transplantation of human fetal cells (10, 11), but limited tissue availability requires alternative cellular sources. Human ES (hES) cells have been transplanted into animal models of PD after in vitro differentiation into neural precursors (12) or DA neurons (13, 14), and partial functional recovery was observed in some of these reports (12, 13). One study reported complete functional recovery after transplantation of differentiated hES cells but severe graft overgrowth was found in engrafted animals (15), emphasizing efforts to purify hES cell-derived neurons via FACS before transplantation (16, 17).

We have recently derived several iPS cell lines from patients with idiopathic PD, which are able to differentiate into DA neurons in vitro (7). Here, we applied a series of transplantation experiments on these PDiPS cell lines to first investigate the development and integration of PD patient iPS (PDiPS) cell-derived neurons in vivo and second to analyze if PDiPS cell-derived DA neurons can function in an animal model of PD.

Results

PDiPS Cells Differentiate into DA Neurons in Vitro and Survive After Transplantation into the Adult Striatum of Unlesioned Rats. We have generated several PDiPS cell lines by transduction of dermal fibroblasts with DOX-inducible lentiviruses encoding oct4, klf4, and sox2 and have described in vitro characteristics of pluripotency and differentiation in these lines (7). We used two PDiPS cell lines, in which the reprogramming factors had been excised after reprogramming (FF17-5 and FF21-26 PDiPSCs; Table 1) (7). In addition, two different PDiPS cell lines from two other patients with PD were used, in which the reprogramming factors were present but their expression not induced (K1 and S1 PDiPS cells; Table 1) (7).

We first analyzed the potential of the four PDiPS cell lines to differentiate into DA neurons in vitro (Fig. S1) using the stromal feeder cell-based differentiation protocol (14, 18). Consistent with our previously published findings from other PDiPS cell lines (7), we did not observe major differences in DA differentiation when comparing the factor-carrying and the factor-free PDiPS cells with hES cells or non-PDiPS cells that had been derived from a subject who did not have PD (Fig. S1). However, one of the PDiPS

Author contributions: G.H., R.J., and O.I. designed research; G.H., O.C., M.D., A.L., K.L., E.M., A.Y., F.S., D.H., and T.O. performed research; F.S., D.H., and O.I. contributed new reagents/analytic tools; G.H., O.C., M.D., A.L., P.J.H., and O.I. analyzed data; and G.H., R.J., and O.I. wrote the paper.

The authors declare no conflict of interest.

¹To whom correspondence may be addressed. E-mail: jaenisch@wi.mit.edu or isacson@hms.harvard.edu.

This article contains supporting information online at www.pnas.org/lookup/suppl/doi:10.1073/pnas.1010209107/-DCSupplemental.

Table 1. Summary of cell lines analyzed in this study

ES/iPS cells studied	H9	A6	K1	S1	FF 17-5	FF 21-26
Cell type	hESC	Non-PDiPSC	PDiPSC	PDiPSC	PDiPSC	PDiPSC
Original cell code (7)	H9	iPS A6	iPS PDA ^{3F} -1	iPS PDC ^{3F} -1	PDB ^{3F} -17Puro-5	PDB ^{3F} -21Puro-26
Parental cell line*	—	GM 01660	AG 20443	AG 20446	AG 20442	AG 20442
Dox-inducible lentivirus	—	Yes	Yes	Yes	Yes	Yes
Reprogramming factors	—	Oct4	Oct4	Oct4	Oct4	Oct4
	—	Klf4	Klf4	Klf4	Klf4	Klf4
	—	Sox2	Sox2	Sox2	Sox2	Sox2
Excision of reprogramming factors	—	No	No	No	Yes	Yes
	—	—	—	—	Factor-free	Factor-free

*Coriell Institute code.

cell lines (S1 PDiPSC) showed an enhanced overall neuronal differentiation but no tendency toward enhanced DA differentiation at day 42 in vitro (Fig. S1). In all stem cell lines, less than 1% of all tyrosine hydroxylase (TH)-positive neurons coexpressed dopamine- β -hydroxylase (DBH), showing that the vast majority of TH⁺ neurons were DA, and not noradrenergic, neurons.

Next, differentiated K1, S1, FF17-5, and FF21-26 PDiPS cells were transplanted into the striatum of unlesioned rats to analyze if engrafted PDiPS cell-derived DA neurons could survive in the adult brain. Four weeks after transplantation, engrafted cells were visualized through a staining against the neural cell adhesion molecule NCAM using a human-specific antibody (Fig. 1A). Viable grafts were found at the expected stereotaxic position in 25 of 26 animals and the mean volumes of the grafts were $0.26 \pm 0.03 \text{ mm}^3$ (K1), $0.60 \pm 0.18 \text{ mm}^3$ (S1), $1.60 \pm 0.56 \text{ mm}^3$ (FF17-5), and $0.44 \pm 0.05 \text{ mm}^3$ (FF21-26). Observed differences in these small graft sizes were most likely a result of variabilities in cell preparation and cell batches for transplantation, as cells from one single differentiation batch were implanted for each PDiPS cell group. Grafts from all four PDiPS cell lines contained human NCAM (hNCAM)-positive and TH⁺ DA neurons at a mean density of 122 ± 24 DA neurons per mm^3 , which were located at the center and periphery of the transplants (Fig. 1B). To analyze longer survival times, we retained five rats with engrafted K1 PDiPS cells and five rats with FF21-26 PDiPS cells from the same series for an additional 8 wk. In all 10 animals, we found viable grafts with DA neurons (Fig. 1C and D). Some of these DA neurons stained positive for Girk-2, which is coexpressed with TH in mesencephalic DA neurons (Fig. 1C and D). Next, the PDiPS cell grafts were stained for β III-tubulin, ubiquitin, and α -synuclein to analyze if engrafted neurons showed any signs of inclusion body formation. We did not detect any ubiquitin-positive and α -synuclein-positive inclusion bodies in PDiPS cell-derived DA and non-DA neurons in any of the grafts analyzed up to 12 wk after transplantation.

The transplantation of differentiated PDiPS cells induced a very modest astrogliosis around the grafts (Fig. 1E). A small number of engrafted cells was found to be GFAP-positive astrocytes (Fig. 1E), whereas the expression of the neural cell adhesion molecule L1, expressed on postmitotic neurons, was abundant in the grafts (Fig. 1F). None of the 36 rats engrafted with differentiated K1, S1, FF17-5, and FF21-26 PDiPS cells showed signs of tumor formation up to 12 wk after transplantation.

Engrafted PD Patient-Derived Neurons Send out Non-DA Axonal Projections to Close and Remote Target Areas in the Adult Unlesioned Rodent Brain. Given that the majority of the neurons in PDiPS cell grafts are non-DA, we investigated other than DA neuronal cell types in the grafts using this in vivo bioassay. For comparison, differentiated non-PDiPS cells and hES cells were transplanted into the striatum of unlesioned rats, and grafts were analyzed 4 wk after transplantation. As an indirect way to ana-

lyze non-DA neuronal phenotypes within the grafts, we followed the fiber outgrowth of hNCAM⁺ neurons throughout the adult rodent brain since engrafted neurons are known to project to their target areas according to their intrinsic phenotypic de-

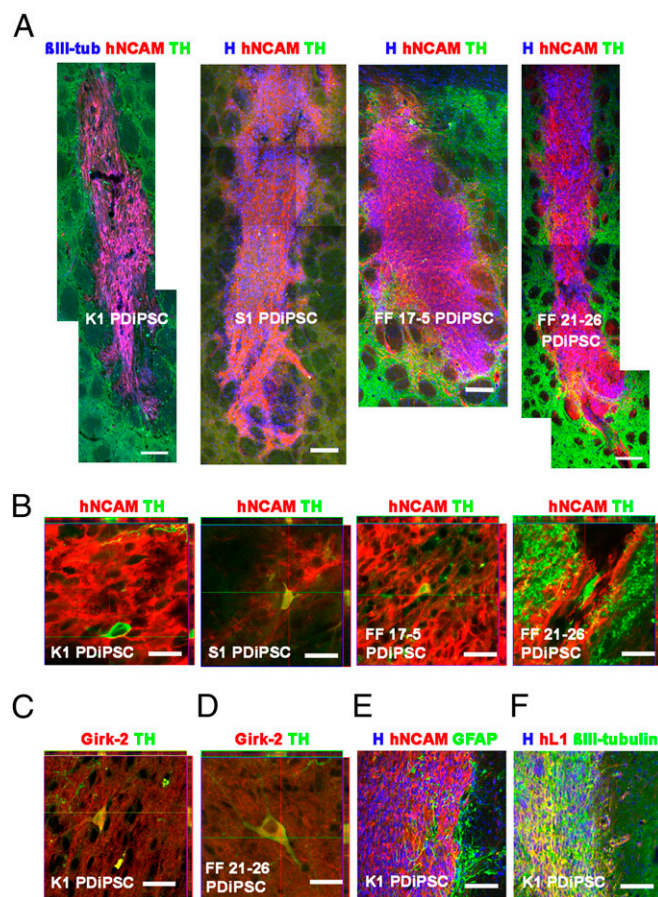


Fig. 1. PD patient-derived DA neurons survive after transplantation into the adult striatum of unlesioned rats. (A) Assembled images of K1, S1, FF 17-5, and FF 21-26 PDiPS cell grafts immunostained for human NCAM (red), TH (green), β III-tubulin (blue), or Hoechst (H; blue) 4 wk after intrastriatal transplantation of 200,000 cells. A high number of neurons was present in all grafts. (B) Z-stacks of three confocal images of 1 μm thickness show coexpression of TH (green) and hNCAM (red) in engrafted DA neurons derived from all four PDiPS cell lines 4 wk after transplantation. (C and D) Stacked confocal images of DA neurons coexpressing Girk-2 (red) and TH (green) 12 wk after transplantation. (E) Immunostaining for hNCAM (red), GFAP (green), and H (blue) showing moderate astrogliosis around grafts. (F) Immunostaining for human L1 (red), β III-tubulin (green) and H (blue) showing a high number of neurons at the graft-host interface. (Scale bars: 100 μm in A, E, and F; 20 μm in B–D.)

termination, as previously shown in several xenografting experiments (19–21). Grafts consisting of all PDiPS cell lines or control lines contained hNCAM⁺ cells, which sent projections to the surrounding gray and white matter (Fig. 2 and Fig. S2). The neurite outgrowth pattern was examined systematically in all six groups, and specific and reproducible patterns were found within each group. These outgrowth patterns were similar for the four PDiPS cell, the non-PDiPS cell, and the hES cell groups (Fig. 2 A–R). A complete list of gray matter zone target areas is shown in Table S1.

As some neurite outgrowth patterns were reminiscent of an outgrowth pattern of cortical projection neurons, we analyzed the expression of the cortical transcription factor *bhlhb5* in the grafts 4 wk after transplantation (Fig. 2 S–U). In all groups, we found small groups of *bhlhb5*⁺ and hNCAM⁺ cortical neurons

(<1%), but we did not detect any differences in *bhlhb5* expression between the PDiPS, the non-PDiPS, and the hES cell grafts.

The lack of differences in donor axon target patterns among the six groups led us to analyze quantitative changes in graft-derived hNCAM⁺ fibers within the different target areas in the host brain. Therefore, we determined the fiber outgrowth per area in 40- μ m brain sections as listed in Table S1. Although slight differences were found in distinct brain areas among the six groups, we did not detect any patterns that indicated PD cell- or iPS cell-specific changes in axonal outgrowth or density between the cell lines.

Analysis of PDiPS Cell-Derived DA Neurons in 6-hydroxydopamine-Lesioned Rats. As the engrafted PDiPS cell-derived DA neurons survive in the adult rodent brain for at least 12 wk, we next transplanted differentiated S1 PDiPS cells into the dorsolateral striatum of 6-hydroxydopamine (6-OHDA)-lesioned rats ($n = 12$), which serve as an animal model of PD, and grafts were analyzed histologically 16 wk after transplantation (Fig. 3). As in the previously described bioassays, the grafts were located at the expected stereotaxic position except for one graft that reached into the globus pallidum (Fig. 3B). All grafts contained a high number of DA neurons ($4,890 \pm 640$) that were distributed throughout the grafts (Fig. 3A–F). Consistent with our *in vitro* data, less than 1% of TH⁺ neurons coexpressed DBH as a marker for noradrenergic neurons (Fig. 3N). The engrafted DA neurons sent TH⁺ fibers toward other cells within the grafts and some of the DA neurons showed intense arborization and branching (Fig. 3C–E).

We next analyzed the outgrowth of DA neurons at the graft/host interface and found that only few donor-derived DA neurons sent their axons toward the DA-depleted host striatum (Fig. 3G). We also analyzed if an astroglial or a microglial reaction was present around the grafts as such reactions could influence graft/host connectivity. Only a small number of astroglial and microglial cells was found around the grafts (Fig. 3H and I).

Next, engrafted DA neurons were stained for the midbrain DA neuronal markers *Girk-2* and *calbindin* (Fig. 3J–L). As seen in the *in vivo* bioassays, we found TH- and *Girk-2*-coexpressing DA neurons within the grafts (Fig. 3J and L). Such neurons accounted for $53.4 \pm 6.6\%$ of all engrafted DA neurons (Fig. 3M). In addition, TH⁺ and *calbindin*-positive DA neurons were also present in the grafts ($6.6 \pm 0.2\%$ of all engrafted DA neurons; Fig. 3J, K, and M). Furthermore, the grafts contained a small number of TH⁺ and GABA⁺ forebrain DA neurons ($4.7 \pm 1.0\%$) and TH⁺ and Nkx2.1⁺ hypothalamic DA neurons ($5.8 \pm 1.2\%$). An immunostaining for TH and α -synuclein showed that the engrafted DA neurons did not contain any α -synuclein-positive inclusion bodies (Fig. 3O–Q). Instead, a punctate synaptic expression pattern of α -synuclein was found in donor-derived neurons within the grafts and also in the host striatum.

None of the 12 animals with S1 PDiPS cell grafts showed signs of tumor formation, and the mean size of the grafts was 1.1 ± 0.08 mm³. Among all engrafted cells, $0.09 \pm 0.02\%$ were positive for the proliferative marker Ki-67 and $83.1 \pm 8.2\%$ of these cells coexpressed hNCAM. Neither SSEA-4- nor oct4-expressing cells were found in the grafts 16 wk after transplantation.

Reduced Motor Asymmetry of 6-OHDA-Lesioned Rats After Intra-striatal Transplantation of differentiated PDiPS Cells. To analyze if the PDiPS cell-derived DA neurons were also functional *in vivo*, rotational tests, a cylinder test, and an adjustment stepping test were performed on all 12 transplanted rats, and their behavioral performance was compared with 6-OHDA-lesioned control rats that had not received any transplants ($n = 9$; Fig. 4). Before surgery, all rats showed severe motor asymmetry induced by both DA agonists, which did not improve in control rats over time (Fig. 4A and D). In contrast, PDiPS cell-transplanted rats showed a progressive reduction in ipsilateral amphetamine-induced ro-

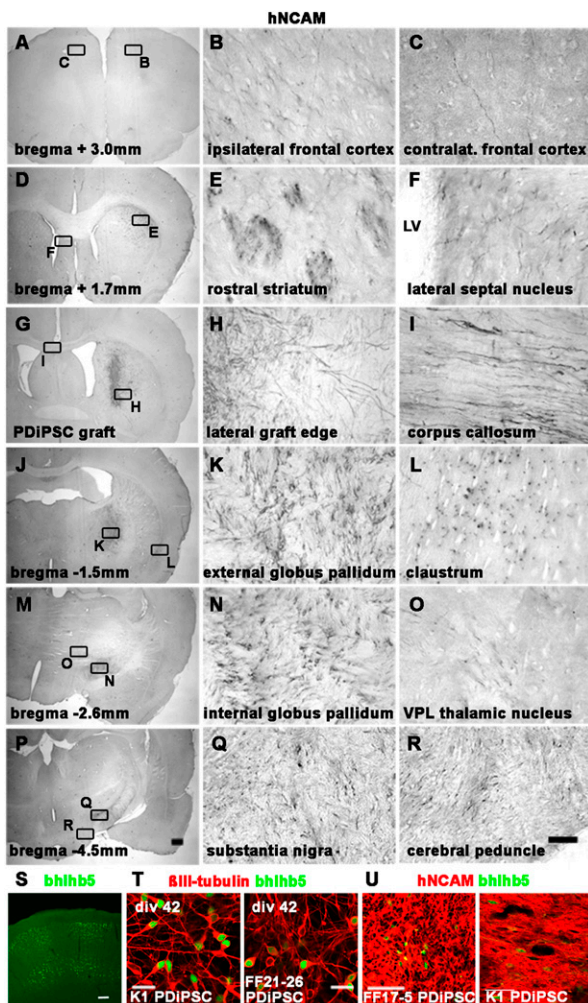


Fig. 2. Engrafted PD patient-derived neurons send out fibers to close and remote target areas in the adult unlesioned rodent brain. (A–R) Photomicrographs of hNCAM-stained brain sections 4 wk after engraftment of S1 PDiPS cells representing the axonal outgrowth pattern of engrafted PDiPS cell-, non-PDiPS cell-, and hES cell-derived neurons. Graft-derived axons project along white matter tracts (E, I, and R) to specific gray matter zone target areas in the adult rodent brain. The boxed areas (Left) are also shown in higher magnification (Right). (Scale bars: 25 μ m, Right; 500 μ m, Left.) LV, lateral ventricle; VPL, ventroposterolateral. (S) Immunostaining of the adult rat somatosensory cortex for the cortical marker *bhlhb5*. (Scale bar: 100 μ m.) (T) Immunostainings of differentiated PDiPS cells at day 42 *in vitro* for β III-tubulin (red) and *bhlhb5* (green). (Scale bar: 20 μ m.) (U) Immunostainings of differentiated PDiPS cells for hNCAM (red) and *bhlhb5* (green) 4 wk after transplantation. (Scale bar: 50 μ m.)

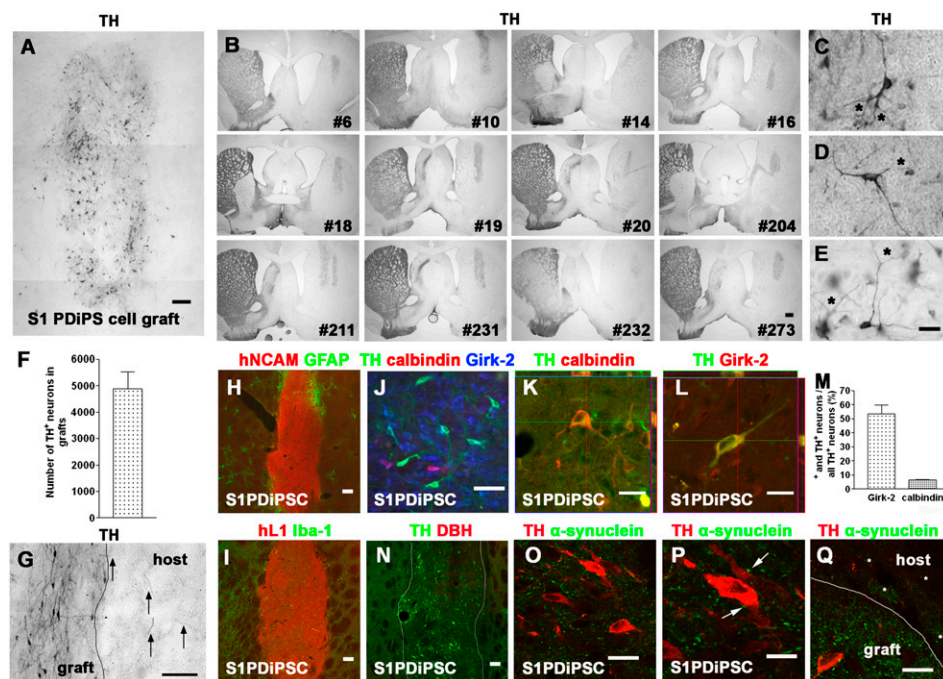


Fig. 3. PDiPS cell-derived DA neurons survive at high numbers after transplantation into the striatum of 6-OHDA-lesioned rats. (A–E and G) Photomicrographs of engrafted differentiated S1 PDiPS cells immunostained for TH 16 wk after transplantation of 400,000 cells into 6-OHDA-lesioned rats. (A) TH⁺ DA neurons were present at high numbers throughout the PDiPS cell grafts. Three images were assembled for graft reconstruction. (B) Low-power photomicrographs show that all 12 transplanted rats contained TH⁺ grafts in the DA-depleted striatum. Numbers indicate individual rats. (C–E) DA neurons with fiber arborization and branching (asterisks) in grafts. (F) Quantification of DA neurons in PDiPS cell grafts. (G) Some graft-derived TH⁺ fibers (arrows) project into the host lesioned striatum. (H) Immunostainings of grafts for hNCAM (red) and GFAP (green) and (I) for hL1 (red) and Iba-1 (green) show low astroglial and microglial reaction around the grafts. (N) Immunostaining of engrafted cells for TH (green) and DBH (red) showing DA, although not noradrenergic, neurons in grafts. (J–M) Girk-2 and calbindin were expressed in engrafted DA neurons. (J) Immunostaining of engrafted cells for TH (green), calbindin (red), and Girk-2 (blue). (K and L) Z-stacks of three confocal images show coexpression of (K) TH (green) and calbindin (red) or (L) TH (green) and Girk-2 (red) in engrafted DA neurons. (M) Quantification of stainings for TH, calbindin, and Girk-2 in PDiPS cell grafts. (O–Q) Immunostainings for TH (red) and α -synuclein (green; human-specific antibody) show a punctate synaptic expression of α -synuclein on engrafted TH⁺ neurons (arrows, P) and in the host striatum (asterisks, Q). (Scale bars: 10 μ m in P; 20 μ m in K, L, O, and Q; 25 μ m in C–E; 50 μ m in J; 100 μ m in A, G, H, I, and N; 500 μ m in B.)

tations up to 16 wk after transplantation (Fig. 4 A–C). The number of rotations was significantly lower compared with the control group at this time point (Fig. 4A). Nine of 12 animals showed a significant reduction in amphetamine-induced rotations at 16 wk after transplantation (Fig. 4B and C). The apomorphine-induced rotation test evaluates the effect of engrafted DA neurons on 6-OHDA-induced hypersensitivity of striatal DA receptors. We found that transplanted rats showed a significantly reduced number of contralateral rotations 16 wk after engraftment compared with the control group (Fig. 4D). The cylinder test and the adjustment stepping test evaluate the connectivity of engrafted DA neurons with host striatal neurons, which control complex motor functions. Consistent with our findings on the limited outgrowth of implanted DA neurons, we did not detect an improved performance in either of these tests in the PDiPS cell-transplanted group compared with the control group at 16 wk after transplantation (Fig. S3).

We next applied FACS for NCAM on differentiated S1 and FF21-26 PDiPS cells before transplantation to further reduce the risk of tumor formation and to examine if the sorted DA neurons would survive in adult rodent brain (Fig. 4 E–G and Fig. S4). Five lesioned rats were transplanted with sorted PDiPS cells and grafts were analyzed at 8 wk ($n = 1$) and 16 wk ($n = 4$) after transplantation. The sorted PDiPS cell grafts were positive for hNCAM and hL1, and none of the grafts showed signs of tumor formation (Fig. 4E and Fig. S4). In all grafts, surviving DA neurons were found at a mean number of 344 ± 92 DA neurons per graft. Probably because of relatively small graft sizes and limited axonal outgrowth, effects on apomorphine-induced ro-

tational asymmetry were not significant and were observed in only one animal 16 wk after transplantation (Fig. S4). However, all animals transplanted with sorted PDiPS cells showed a significant reduction of amphetamine-induced rotations at 16 wk after transplantation compared with control animals ($n = 5$), which did not improve over time (Fig. 4G and Fig. S4).

Discussion

The application of patient-derived iPS cells for cell therapy has the advantage of using genetically identical cells, which can be introduced into a patient without the need for immunosuppression. Here, we differentiated iPS cell lines from three patients with sporadic PD into DA neurons and applied a series of in vivo experiments on these cells. We used cell transplantation as a long-term in vivo bioassay on PDiPS cells, which provides opportunities to study cell development, neuronal maturation, and neuronal cell survival, and importantly, allows evaluation of potential degenerative changes in a physiological 3D context over a prolonged time period. In all PDiPS cell groups, we found viable grafts for at least 12 wk after transplantation that stained positive for hNCAM and hL1. None of the PDiPS cell-derived neurons showed signs of inclusion body formation or other morphological features that would indicate a neurodegenerative process in the cells. An analysis of the axonal outgrowth of engrafted neurons derived from PDiPS cells, non-PDiPS cells, and hES cells revealed a specific and reproducible pattern, which was highly conserved within and between groups. These data show that permissive guidance cues for developing axons are still present in the adult rodent brain, and that the implanted human iPS and ES cell-derived

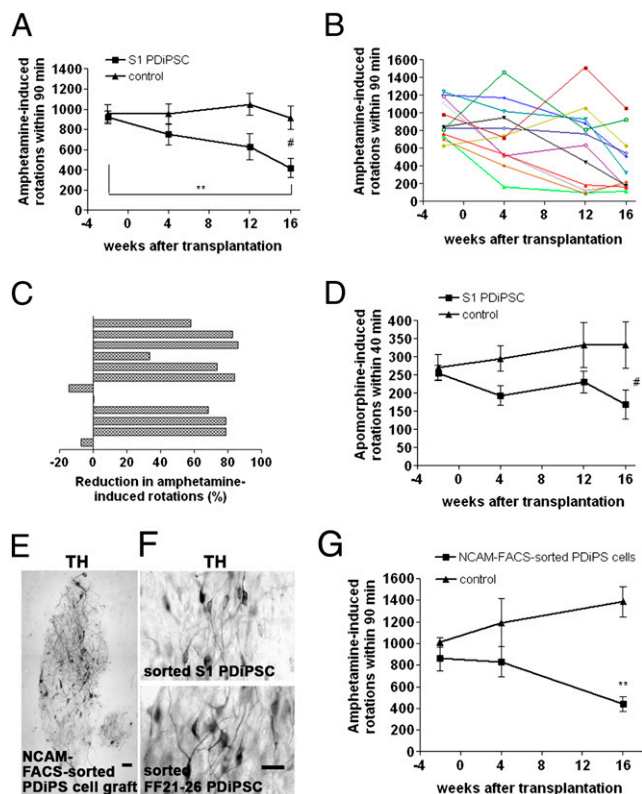


Fig. 4. Reduced motor asymmetry of 6-OHDA-lesioned rats after intrastriatal transplantation of differentiated PDiPS cells. (A–C) Amphetamine-induced rotations of S1 PDiPS cell-transplanted rats ($n = 12$) significantly declined over time (** $P < 0.01$) and were significantly less compared with control rats ($n = 9$) 16 wk after transplantation ($\#P < 0.05$). (B) Number of rotations of each rat over time. (C) The percentage of the reduction in rotations 16 wk after transplantation. (D) Apomorphine-induced rotations of rats over time reveal a significantly decreased number of rotations in PDiPS cell-treated rats 16 wk after transplantation compared with control rats ($\#P < 0.05$). (E–G) Differentiated S1 and FF21-26 PDiPS cells were FACS-sorted for NCAM and subsequently engrafted into five 6-OHDA-lesioned rats (S1, $n = 2$; FF21-26, $n = 3$). (E and F) Photomicrographs of TH⁺ DA neurons 16 wk after transplantation. Three images were assembled in panel E for graft reconstruction. (Scale bars: 50 μm in E; 25 μm in F.) (G) The number of amphetamine-induced rotations of rats engrafted with sorted PDiPS cells was significantly lower compared with control rats ($n = 5$) 16 wk after transplantation (** $P < 0.01$). Graphs show mean values \pm SEM. Two-way ANOVA with post hoc Tukey test was performed for statistical analysis.

neurons were responsive to these guidance cues independent of the ES or PD donor cell origin. It has previously been demonstrated in xenografting experiments that engrafted donor neurons project to their target areas according to their intrinsic phenotypic determination (19–21). In this study, several brain areas were specifically innervated by implanted cells, which indicates that different neuronal phenotypes, including cortical projection neurons, had survived in the grafts. Although we could not detect PD-related changes in axonal fiber outgrowth, other parameters such as axonal transport, synaptogenesis, synaptic pruning, or synaptic function could be further analyzed for PD-related changes by applying such an *in vivo* bioassay. In addition, observation periods could be further prolonged for up to 2 to 3 y to evaluate any disease-related changes, which might occur outside the time window described in this study, and other host models including SCID mice (22) could be considered, which do not require the application of immunosuppressive agents.

The initial transplantation experiments in this study showed that DA neurons survived in all unlesioned animals of the PDiPS

cell groups for many months after transplantation. We therefore transplanted differentiated PDiPS cells into the striatum of 6-OHDA-lesioned rats as a functional and behavioral model for PD. In all animals, viable grafts with a high number of DA neurons without signs of neurodegeneration were found 16 wk after transplantation, and the survival rate of these DA neurons—an indirect measure for cell vulnerability—was comparable to those shown in studies on engrafted differentiated hES cells (13) or primate ES cells (23) 16 to 20 wk after transplantation. The PDiPS cell-derived DA neurons showed functional effects as demonstrated by a significant reduction in amphetamine- and apomorphine-induced rotations 16 wk after transplantation. Nine of 12 animals showed a significant reduction in amphetamine-induced asymmetry and the degree of behavioral improvement reached more than 70% in the majority of these rats. One rat without improvement had a misplaced graft that reached into the globus pallidum, and another rat presented with an unusually wide ventricular system. Although the reduction of motor asymmetry was prominent, a full recovery was not observed up to 16 wk after transplantation. This is possibly because of the long maturation process that human DA neurons have to undergo *in vivo*, as reported in studies on implanted human mesencephalic DA neurons that show a significant reduction in amphetamine-induced rotation at 15 wk, but only full recovery by 20 wk after transplantation (24). Given that the transplanted rats improved gradually over time, more pronounced effects might have occurred if the rats had been analyzed for a longer period after transplantation. We did not detect any effects in cylinder and adjustment stepping tests, which is probably a result of the observed poor outgrowth of implanted PDiPS cells to host neurons in the striatum. Reduced outgrowth of DA neurons has previously been described for both implanted differentiated mouse (25) and human (13) ES cells and is therefore unlikely to be PD- or iPS cell-related. This is supported by the fact that we could not detect PD- or iPS cell-related differences in axonal outgrowth of engrafted neurons in our *in vivo* bioassays. Increasing the number of cells for transplantation and further improvements of the differentiation protocol might lead to better functional outcomes. Approximately 50% of the engrafted PDiPS cell-derived DA neurons coexpressed *Girk-2*, which, together with TH, is typically expressed in substantia nigra (A9) DA neurons that project into striatal tissue. However, only a few graft-derived DA axons were found to innervate the host striatum, indicating a heterogeneous population of engrafted *Girk-2*- and TH-coexpressing DA neurons. Indeed, a subset of other neurons outside the A9 region also coexpress TH and *Girk-2* (26) and the engrafted PDiPS cell-derived DA neurons did not coexpress the transcription factor *foxA2* that is found together with TH in most A9 midbrain DA neurons (27). Therefore, we believe the PDiPS cells have most likely been inefficiently patterned toward an A9 DA neuronal phenotype during *in vitro* differentiation. Notably, hES cell-derived DA neurons also have not yet been shown to coexpress TH and *foxA2* after transplantation using different differentiation protocols, including ours (12–15), indicating that new strategies toward phenotypic patterning of hES and hiPSs cells during *in vitro* differentiation have to be pursued. During the course of this study, however, we and others have developed protocols that generate *foxA2*⁺ floor plate cells from hES cells (28) or *foxA2*⁺ DA neurons from hES and PDiPS cells *in vitro* (29), which provide encouraging cell sources for future transplantation studies to further improve axonal outgrowth and behavioral outcomes.

None of the 48 PDiPS cell grafts analyzed in this study showed signs of tumor formation up to 16 wk after transplantation. However, we and others have previously shown that tumor formation can occur when transplanting human pluripotent stem cell-derived cells (14, 15), demonstrating a requirement to further purify cells before transplantation. Therefore, we performed FACS of differentiated PDiPS cells for NCAM before transplantation and

did not observe signs of tumor formation in the grafts. Instead, NCAM-purified DA neurons had survived in all grafts, which also showed functional effects on amphetamine-induced rotational asymmetry. Interestingly, engrafted factor-carrying PDiPS cells did not express oct4 at 16 wk after transplantation. Oct4 is one of the factors used during derivation of PDiPS cells (7) indicating that sufficient gene silencing is possible in engrafted iPS cells. However, factor-free PDiPS cells constitute a safer cell source for cell replacement approaches, and therefore we have characterized these cells along with factor-carrying PDiPS cells in this study. Future clinical applications will likely demand new techniques for generating factor-free iPS cells such as virus-free (30) or DNA-free approaches (31) at acceptable efficiencies.

The present study provides a basis for future comparative studies on iPS cell lines from patients with genetic PD (genPDiPS cells). Mutations in the PD-related genes LRRK2 or α -synuclein have been linked to an impairment of neurite outgrowth (32, 33) that, together with potential inclusion body formation or potential changes in DA cell survival, could be evaluated in a physiological context in long-term in vivo bioassays as described here. Such in vivo bioassays can be further applied to analyze function of genPDiPS cells in vivo, to test new drugs on engrafted genPDiPS cells, or to validate any in vitro gene targeting approaches that might be necessary in genPDiPS cells before they can be considered for applications in vivo. Importantly, the present study provides a proof of principle that engrafted PDiPS cells can have functional effects in an animal model of PD. At the same time, it encourages to further improve differentiation protocols and cell purification methods, as well as strategies to generate patient-specific iPS cells for future clinical applications.

Methods

In Vitro Differentiation of Human Stem Cells. Human stem cells were maintained on mitomycin C-inactivated human D551 fibroblasts (American Type Culture Collection) and were differentiated according to a stromal feeder cell-based protocol (18), which was modified through the addition of noggin (300 ng/mL) during the first 21 d of differentiation to improve neuroectodermal differentiation (14).

Cell Transplantation and Behavioral Analysis. All animal procedures were performed according to National Institutes of Health guidelines and were approved by the Institutional Animal Care and Use Committee at McLean Hospital and Harvard Medical School. Differentiated cells were harvested at day 42 in vitro and transplanted into the striatum of adult Sprague-Dawley rats at a density of 100,000 viable cells per microliter. The surgical procedures and behavioral tests have been described in detail (14, 23). Amphetamine and apomorphine were applied at doses of 4 mg/kg i.p. or 0.1 mg/kg s.c., respectively. Data were analyzed using Statistica software (StatSoft).

Immunohistochemistry and Cell Counts. Immunostainings of brain sections were performed as previously described (14, 23). Cell counts of DA neurons in 6-OHDA-lesioned rats were obtained by applying the fractionator probe. Only TH⁺ cells with visible neurites were counted. A detailed description of all methods can be found in *SI Methods*.

ACKNOWLEDGMENTS. We thank Andrew Kartunen for excellent technical help. This study was supported by the Udall Parkinson's Disease Center of Excellence Grant P50 NS39793 (to O.I.), Michael Stern Foundation Grant WX81XVW-05-1-0555 (to O.I.), Parkinson's Disease iPS Cell Line Research Consortium Grant 1RC2NS070276-01 (to O.I.), Orchard Foundation (O.I.), the Consolidated Anti-Aging Foundation (O.I.), Harold and Ronna Cooper Family (O.I.); National Institutes of Health Grants R01-HD045022 (to R.J.) and R01 CA098959-01 (to R.J.), a Collaborative Innovation Award from the Howard Hughes Medical Institute (R.J.), postdoctoral fellowship HA5589/1-1 from the Deutsche Forschungsgemeinschaft (to G.H.), and Training Award T32AG000222-17 from the National Institute on Aging (to T.O.). D.H. is a Merck Fellow of the Life Science Research Foundation.

- Takahashi K, Yamanaka S (2006) Induction of pluripotent stem cells from mouse embryonic and adult fibroblast cultures by defined factors. *Cell* 126:663–676.
- Saha K, Jaenisch R (2009) Technical challenges in using human induced pluripotent stem cells to model disease. *Cell Stem Cell* 5:584–595.
- Wernig M, et al. (2008) Neurons derived from reprogrammed fibroblasts functionally integrate into the fetal brain and improve symptoms of rats with Parkinson's disease. *Proc Natl Acad Sci USA* 105:5856–5861.
- Raya A, et al. (2009) Disease-corrected haematopoietic progenitors from Fanconi anaemia induced pluripotent stem cells. *Nature* 460:53–59.
- Park IH, et al. (2008) Disease-specific induced pluripotent stem cells. *Cell* 134:877–886.
- Maehr R, et al. (2009) Generation of pluripotent stem cells from patients with type 1 diabetes. *Proc Natl Acad Sci USA* 106:15768–15773.
- Soldner F, et al. (2009) Parkinson's disease patient-derived induced pluripotent stem cells free of viral reprogramming factors. *Cell* 136:964–977.
- Ebert AD, et al. (2009) Induced pluripotent stem cells from a spinal muscular atrophy patient. *Nature* 457:277–280.
- Lee G, et al. (2009) Modelling pathogenesis and treatment of familial dysautonomia using patient-specific iPSCs. *Nature* 461:402–406.
- Astradsson A, Cooper O, Vinuela A, Isacson O (2008) Recent advances in cell-based therapy for Parkinson disease. *Neurosurg Focus* 24:E6.
- Lindvall O, Kokaia Z (2009) Prospects of stem cell therapy for replacing dopamine neurons in Parkinson's disease. *Trends Pharmacol Sci* 30:260–267.
- Ben-Hur T, et al. (2004) Transplantation of human embryonic stem cell-derived neural progenitors improves behavioral deficit in Parkinsonian rats. *Stem Cells* 22:1246–1255.
- Yang D, Zhang ZJ, Oldenburg M, Ayala M, Zhang SC (2008) Human embryonic stem cell-derived dopaminergic neurons reverse functional deficit in parkinsonian rats. *Stem Cells* 26:55–63.
- Sonntag KC, et al. (2007) Enhanced yield of neuroepithelial precursors and midbrain-like dopaminergic neurons from human embryonic stem cells using the bone morphogenetic protein antagonist noggin. *Stem Cells* 25:411–418.
- Roy NS, et al. (2006) Functional engraftment of human ES cell-derived dopaminergic neurons enriched by coculture with telomerase-immortalized midbrain astrocytes. *Nat Med* 12:1259–1268.
- Pruszk J, Sonntag KC, Aung MH, Sanchez-Pernaute R, Isacson O (2007) Markers and methods for cell sorting of human embryonic stem cell-derived neural cell populations. *Stem Cells* 25:2257–2268.
- Pruszk J, Ludwig W, Blak A, Alaviani K, Isacson O (2009) CD15, CD24, and CD29 define a surface biomarker code for neural lineage differentiation of stem cells. *Stem Cells* 27:2928–2940.
- Perrier AL, et al. (2004) Derivation of midbrain dopamine neurons from human embryonic stem cells. *Proc Natl Acad Sci USA* 101:12543–12548.
- Victorin K, Brundin P, Gustavii B, Lindvall O, Björklund A (1990) Reformation of long axon pathways in adult rat central nervous system by human forebrain neuroblasts. *Nature* 347:556–558.
- Isacson O, et al. (1995) Transplanted xenogeneic neural cells in neurodegenerative disease models exhibit remarkable axonal target specificity and distinct growth patterns of glial and axonal fibres. *Nat Med* 1:1189–1194.
- Isacson O, Deacon TW (1996) Specific axon guidance factors persist in the adult brain as demonstrated by pig neuroblasts transplanted to the rat. *Neuroscience* 75:827–837.
- Shultz LD, Ishikawa F, Greiner DL (2007) Humanized mice in translational biomedical research. *Nat Rev Immunol* 7:118–130.
- Sanchez-Pernaute R, et al. (2008) Parthenogenetic dopamine neurons from primate embryonic stem cells restore function in experimental Parkinson's disease. *Brain* 131:2127–2139.
- Brundin P, et al. (1986) Behavioural effects of human fetal dopamine neurons grafted in a rat model of Parkinson's disease. *Exp Brain Res* 65:235–240.
- Yurek DM, Fletcher-Turner A (2004) Comparison of embryonic stem cell-derived dopamine neuron grafts and fetal ventral mesencephalic tissue grafts: morphology and function. *Cell Transplant* 13:295–306.
- Schein JC, Hunter DD, Roffler-Tarlov S (1998) Girk2 expression in the ventral midbrain, cerebellum, and olfactory bulb and its relationship to the murine mutation weaver. *Dev Biol* 204:432–450.
- Ferri AL, et al. (2007) Foxa1 and Foxa2 regulate multiple phases of midbrain dopaminergic neuron development in a dosage-dependent manner. *Development* 134:2761–2769.
- Fasano CA, Chambers SM, Lee G, Tomishima MJ, Studer L (2010) Efficient derivation of functional floor plate tissue from human embryonic stem cells. *Cell Stem Cell* 6:336–347.
- Cooper O, et al. (2010) Differentiation of human ES and Parkinson's disease iPS cells into ventral midbrain dopaminergic neurons requires a high activity form of SHH, FGF8a and specific regionalization by retinoic acid. *Mol Cell Neurosci*, Jul 23 [published ahead of print].
- Yu J, et al. (2009) Human induced pluripotent stem cells free of vector and transgene sequences. *Science* 324:797–801.
- Kim D, et al. (2009) Generation of human induced pluripotent stem cells by direct delivery of reprogramming proteins. *Cell Stem Cell* 4:472–476.
- MacLeod D, et al. (2006) The familial Parkinsonism gene LRRK2 regulates neurite process morphology. *Neuron* 52:587–593.
- Marongiu R, et al. (2009) Mutant PINK1 induces mitochondrial dysfunction in a neuronal cell model of Parkinson's disease by disturbing calcium flux. *J Neurochem* 108:1561–1574.